GEOLOGIJA. 2008. Vol. 50. Supplement. P. S26–S39
DOI: 10.2478/V10056-008-0022-5

Microstructure and physico-mechanical properties of tills in Poland

Jerzy Trzciński

Trzciński J. Microstructure and physico-mechanical properties of tills in Poland. *Geologija*. Vilnius. 2008. Vol. 50. Supplement. P. S26–S39. ISSN 1392-110X

SEM analysis of the microstructure and physico-mechanical properties of Polish tills was performed. The following microstructural features were examined: the degree of packing of structural elements, the stability of contacts among them, types of contacts between clayey microaggregates as well as the size and shape of pores. Three types of microstructures occur in the analysed tills: skeletal, matrix and matrix-turbulent. According to the degree of packing of the microstructures, three subtypes were distinguished in matrix microstructure: subtype A (loosely packed), subtype B (medium packed) and subtype C (tightly packed). Relations between microstructures types / subtypes and physical-mechanical properties were recognised. There is a noticeable decrease of water content, porosity, soaking and compressibility accompanied by an increase of bulk density, swelling and shear strength from tills with the skeletal microstructure, through tills with the matrix microstructure to those with the matrix-turbulent microstructure. A detailed analysis of relations between the physico-mechanical properties of tills and their microstructure revealed that water contained in pore spaces and some microstructural features have a direct effect on these relations.

Key words: tills, microstructure, physico-mechanical properties, relations

Received 03 March 2008, accepted 06 May 2008

Jerzy Trzciński. Institute of Hydrogeology and Engineering Geology, Warsaw University, Żwirki i Wigury 93, 02-089 Warsaw, Poland. E-mail: Jerzy.Trzcinski@uw.edu.pl

INTRODUCTION

Tills are the most widely distributed Pleistocene deposits of the continental Quaternary glaciations. Tills are also common in Poland, both directly exposed at the surface or covered by other Quaternary deposits. Their thickness ranges from several dozens of centimetres to about a dozen of metres, and occasionally even several tens of metres.

Structure is a term of a very wide meaning frequently used in geology. In engineering geology, structure is understood as a fabric (a term reflecting the size, shape and arrangement of particles and pores), interparticle forces as well as the mineral composition (e. g., Mitchell, 1993). Recognition of the structure is crucial for the interpretation of the physical and mechanical properties of sediments.

Investigations of the physico-mechanical properties of Pleistocene till are carried out by many scientists in different areas of Poland. These investigations are focused on the influence of such factors as moisture, load history, fracturing and weathering on the engineering-geological properties of these deposits (e. g., Falkiewicz, 1962; Kowalski, Lipińska, 1963; Wysokiński, 1967; Krajewska-Pinińska, 1969; Sztromajer, 1982; Kaczyński, Trzciński, 1992; Trzciński, 1998; Trzciński, Kaczyński, 1999; Kaczyński, Trzciński, 2000).

METHODS

The outcrops were selected with regard to the possibilities of sampling soils with natural moisture and a non-disturbed structure. Various kinds of exposures such as foundation pits, mining pits and escarpments of river valleys were examined. In selected outcrops, till samples were taken from the depths of 1.5 m to 10 m below surface. Tills of the North Polish, Mid Polish and South Polish glaciations were examined. During the field works, the sites were subdivided into "reference sites" and "observation sites". The reference sites (31) were represented by large exploitation pits or by valley escarpments. Foundation pits of smaller sizes represented the observation sites (49). The location of the exposures is presented in Fig. 1.

The methodology of microstructure analysis by scanning electron microscopy (SEM) was described in detail by Trzciński (2004) and used in engineering-geological investigations (e. g. Osipov et al., 1984; Kaczyński, Trzciński, 1999; Gratchev et al., 2006) and in the study of till (Ruszczyńska-Szenajch et al., 2003). The samples to be analysed were dried by the freeze-drying method (e. g., Smart, Tovey, 1982). The Hitachi S-800 and Jeol 840A microscopes were used. A qualitative description was completed on the basis of photograph series of two sample surfaces, select-

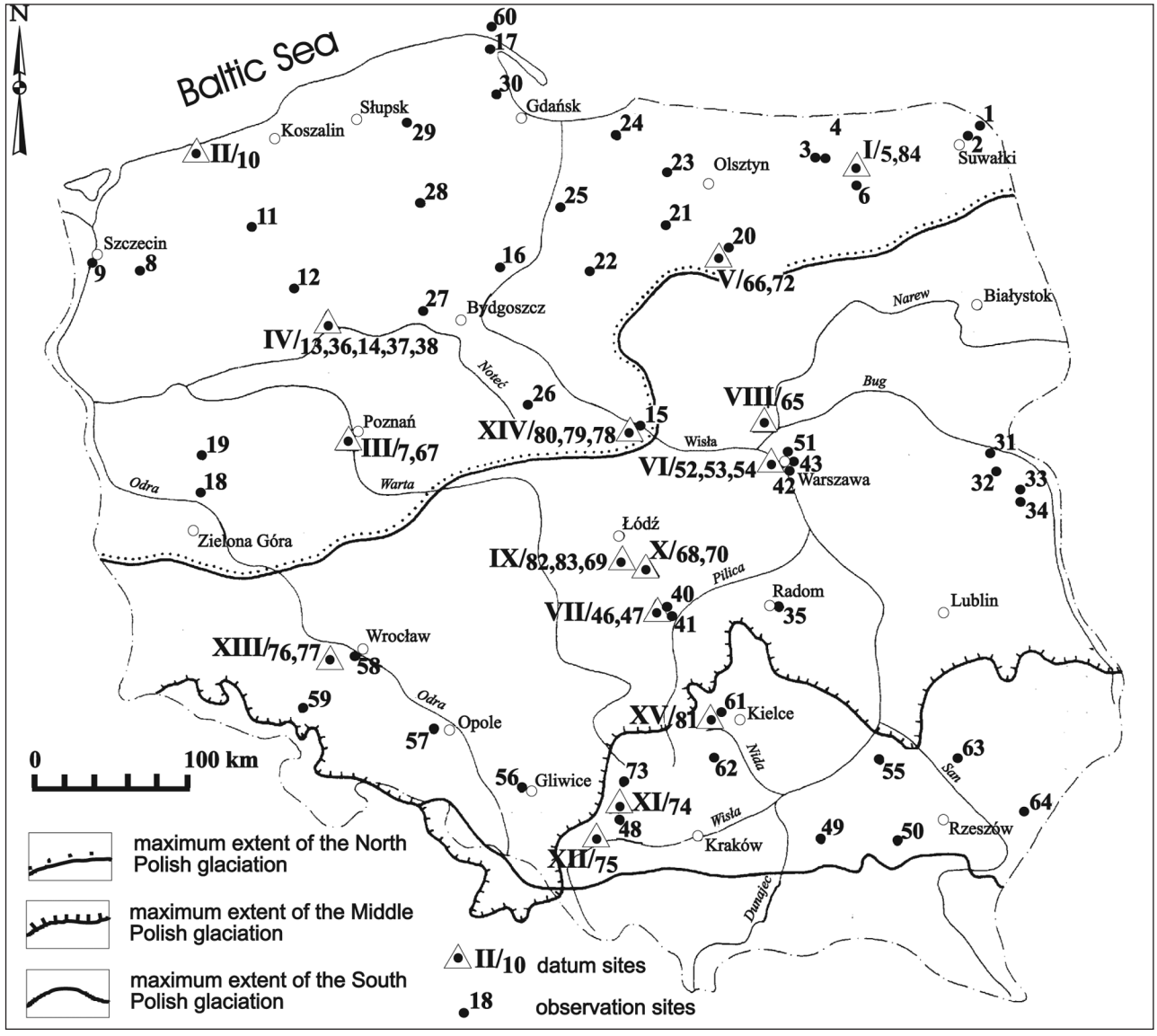

Fig. 1. Location of the exposures; maximum extents of Polish Glaciations according to Lindner (1984): *1* – Puńsk, *2* – Żubryn near Suwałki, *3* – Grajewo near Giżycko, *4* – Grajewo near Giżycko, *I/5* – Ranty, *6* – Orzysz, *III/7* – Poznań, *8* – Stargard Szczeciński, *9* – Szczecin, *II/10* – Włodarka near Trzebiatów, *11* – Jelonki near Połczyn Zdrój, *12* – Wałcz, *IV/13* – Ujście near Piła, *IV/14* – Ujście near Piła, *15* – Kobierniki near Płock, *16* – Trzeciewiec near Bydgoszcz, *17* – Władysławowo, *18* – Sulechów-Brzezie, *19* – Świebodzin, *20* – Turza Wielka near Działdowo, *21* – Lubawa, *22* – Tiwoli near Brodnica, *23* – Wólka Majdańska near Ostróda, *24* – Elbląg, *25* – Kwidzyń, *26* – Strzelno, *27* – Nakło by Noteć river, *28* – Chojnice, *29* – Bytów, *30* – Przodkowo near Kartuzy, *31* – Serpelice, *32* – Wolka Nosowska, *33* – Ossówka, *34* – Hrud, *35* – Radom, *IV/36* – Ujście near Piła, *IV/37* – Ujście near Piła, *IV/38* – Ujście near Piła, *40* – Bełchatów, *41* – Bełchatów, *42* – Warszawa, *43* – Warszawa, *VII/46* – Bełchatów, *VII/47* – Bełchatów, *48* – Mysłowice, *49* – Brzesko, *50* – Pilzno, *51* – Warszawa, *VI/52* – Warszawa, *VI/53* – Warszawa, *VI/54* – Warszawa, *55* – Tarnobrzeg, *56* – Gliwice-Ostropa, *57* – Chróścina near Opole, *58* – Smolec near Wrocław, *59* – Świdnica, *60* – Jastrzębia Góra, *61* – Włoszczowa, *62* – Wodzisław, *63* – Lipiny Dolne, *64* – Oleszyce near Lubaczów, *VIII/65* – Dębe on the Narew river, *V/66* – Turza Wielka near Działdowo, *III/67* – Poznań, *X/68* – Polichno near Piotrków Trybunalski, *IX/69* – Moszczenica, *X/70* – Polichno near Piotrków Trybunalski, *V/72* – Turza Wielka near Działdowo, *73* – Woźniki Śląskie, *XI/74* – Kozłowa Góra near Piekary Śląskie, *XII/75* – Pszczyna-Stara Wieś, *XIII/76* – Zachowice, *XIII/77* – Zachowice, *XIV/78* – Płock Podolszyce, *XIV/79* – Płock Podolszyce, *XIV/80* – Płock Podolszyce, *XV/81* – Bolmin, *IX/82* – Moszczenica, *IX/83* – Moszczenica, *I/84* – Ranty

ing at least two representative areas. The sample surface was then photographed, using 50× to 5000× magnifications.

The methodology of laboratory tests of the physico-mechanical properties of tills was described in detail by Trzciński (1998). Most of these properties (water content, bulk density, dry density, porosity, void ratio and shear strength) were determined according to the methodology given by the Polish building standard (Polska Norma, 1988). The swelling of tills was tested according to the method devised by Grabowska-Olszewska, Kaczyński, 1994 and the degree of slaking according to the methodology of Kaczyński (1981). The consolidation test was carried out in an oedometer and a consolidometer. Procedures suggested in the instruction ITB nos. 288, 289 (Piaskowski, 1989a; 1989b) and given by Scott (1961), Vu Cao Minh, Glazer (1977), Kaczyński (1981), Dobak (1986) were applied to determine the deformation of tills in the consolidometer.

TILL MICROSTRUCTURE

The analysis allowed to determine the presence of three types of microstructure in the tills (according to the classification of Sergeyev et al., 1980; Grabowska-Olszewska et al., 1984): matrix, skeletal, and matrix-turbulent. Taking into account the relative packing of structural elements, three subtypes were determined within the matrix microstructure: subtype A – loosely packed, subtype B – medium packed, and subtype C – tightly packed (Trzciński, 2003). Outcrops with the identified type / subtype of the microstructure are presented in Table 1.

The matrix microstructure (Fig. 2–4) comprises mainly a clayey matrix, with singular sandy grains, and subordinate thicker silty grains. The grain surface is covered with clay particles – a "clay film". In subtype A (Fig. 2), sandy grains are loosely connected with the clayey-silty matrix. Clayey-silty microaggregates of the matrix are loosely packed and randomly distributed. Contacts among the clayey microaggregates are of the face-to-edge type. In subtype B (Fig. 3), the clayey-silty matrix is medium-packed and evenly distributed. The clayey microaggregate contacts are of face-to-face, subordinately of face-to-edge type. In subtype C (Fig. 4), the sandy and silty grains are tightly connected with the clayey matrix. Clay films tightly cover the surfaces of the sandy grains and are closely connected with them. The matrix is tightly packed and evenly distributed. The clayey microaggregate contacts are of the face-to-face type.

The skeletal microstructure (Fig. 5) comprises mainly sandy grains with subordinate coarser silty grains among which clayey and fine silty material is present. The clayey-silty microaggregates are loosely and randomly distributed on the grains of the skeleton or form connections among them. Contacts among the clayey microaggregates are mainly of the face-to-edge type.

The matrix-turbulent microstructure (Fig. 6) comprises a clayey matrix with single sandy and coarser silty grains. Sandy grains are tightly covered with clay films which are tightly connected with them. The structural elements of the matrix are tightly packed, in some cases the clayey microaggregates are turbulently arranged. The clayey microaggregate contacts are frequently of the face-to-face type.

Generally, the structural elements of the skeletal microstructure are loosely packed, and those of the matrix-turbulent microstructure are tightly packed. The matrix microstructure is the most common, while the matrix-turbulent one is the least frequent.

PHYSICO-MECHANICAL PROPERTIES OF TILLS IN RELATION TO THEIR MICROSTRUCTURE

The following parameters were analysed: water content, bulk density, dry density, porosity, void ratio, free swell, slaking, compressibility and shear strength. The results are presented in Tables 2–5 and Figs. 7–9. Values given in Tables are based on all data obtained for tills from all exposures. Average values were used to construct the diagrams.

Table 1. **Compilation of outcrops with identified type / subtype of the microstructure (numbering as in Fig. 1)**

Microstructures Type / subtype		Reference sites (Fig. 1)	Observation sites (Fig. 1)	Number of outcrops	% of outcrops
Skeletal		I/84, V/66, V/72, XIII/77, XV/81	18, 19, 21, 22, 29	10	12
Matrix	A	II/10, III/7, III/67, IV/36, IV/37, VI/52, VII/46, XIV/80	1, 3, 4, 6, 17, 23, 24, 26, 51, 56, 62	19	23
	B	I/5, IV/13, IV/14, VI/53, IX/82, IX/83, XI/74, XII/75, XIII/76	2, 8, 9, 11, 15, 16, 20, 25, 27, 28, 30, 32, 33, 34, 35, 39, 42, 48, 55, 57, 58, 59, 61, 63, 64, 73	35	42
	C	VI/54, VII/47, VIII/65, X/70, XIV/78	12, 31, 40, 41, 43, 44, 45, 49, 50, 60	15	18
Matrix–turbulent		IV/38, IX/69, X/68, XIV/79		4	5

Table 2. **Relation of the physical properties of tills (water content, bulk and dry density, porosity, void ratio) to types/subtypes of their microstructures**

Microstructures Type / subtype			Water content w, %	Bulk density ρ, mg/m³	Dry density ρ_d, mg/m³	Porosity n, %	Void ratio e (–)
Skeletal		R	6.1–25.9	1.75–2.13	1.48–1.97	26.5–45.8	0.36–0.84
		$\overline{X}$	13.5	1.90	1.68	38.0	0.62
Matrix	A	R	9.6–23.1	1.78–2.15	1.49–1.96	26.5–44.6	0.36–0.81
		$\overline{X}$	14.6	1.94	1.70	36.4	0.58
	B	R	7.7–21.6	1.75–2.18	1.44–1.98	24.7–47.4	0.32–0.90
		$\overline{X}$	13.6	2.00	1.75	34.5	0.53
	C	R	7.8–15.9	1.95–2.30	1.72–2.13	22.5–36.3	0.29–0.74
		$\overline{X}$	10.9	2.15	1.94	27.8	0.41
Matrix–turbulent		R	12.1–15.3	2.11–2.19	1.85–1.90	25.2–31.3	0.34–0.45
		$\overline{X}$	13.4	2.14	1.88	29.3	0.42

R – minimum–maximum, $\overline{X}$ – arithmetical mean.

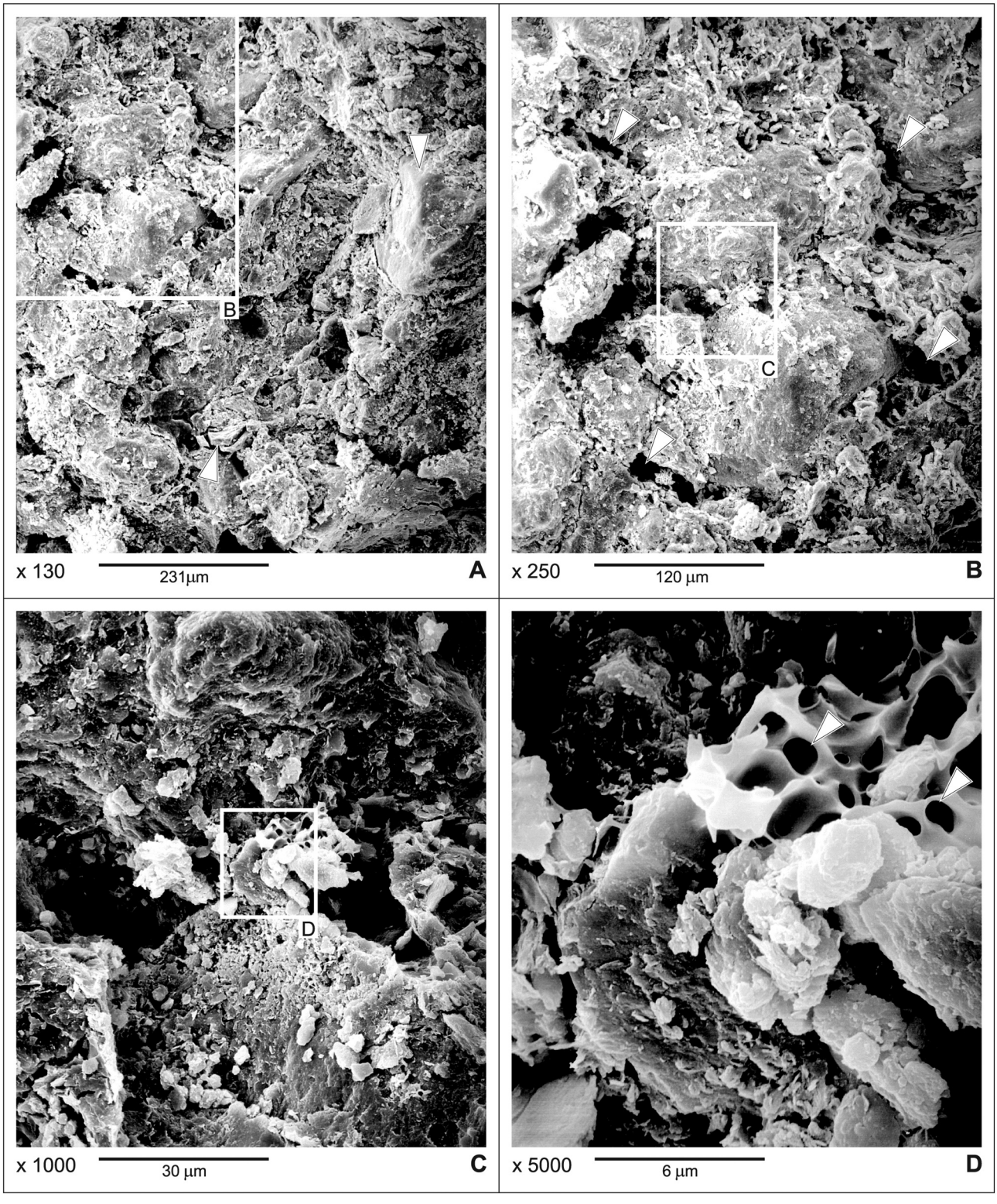

Fig. 2. Scanning electron photomicrographs of the matrix microstructure (subtype A). Microstructure of till from exposure number III/67, location in Fig. 1. Orientation: S–N (S – left part of the photos). *A* – sandy and silty grains (arrows) within a clayey matrix. Grains loosely joined with matrix. The pore space is formed by anisometric and isometric large mesopores (black areas) among the sandy-silty aggregates; *B* – enlarged detail of A: unevenly distributed and loosely packed clayey matrix between sandy grains. The pore space is formed by isometric and anisometric intermicroaggregate micropores (arrows); *C* – enlarged detail of B: microaggregate (in the centre of the photograph) within sandy grains. Intergranular mesopores (black areas) visible on the left and right side of the microaggregate; *D* – enlarged fragment of microaggregate from C: clayey microaggregate. Intraparticle isometric micropores are visible in the upper right part of the photo (arrows)

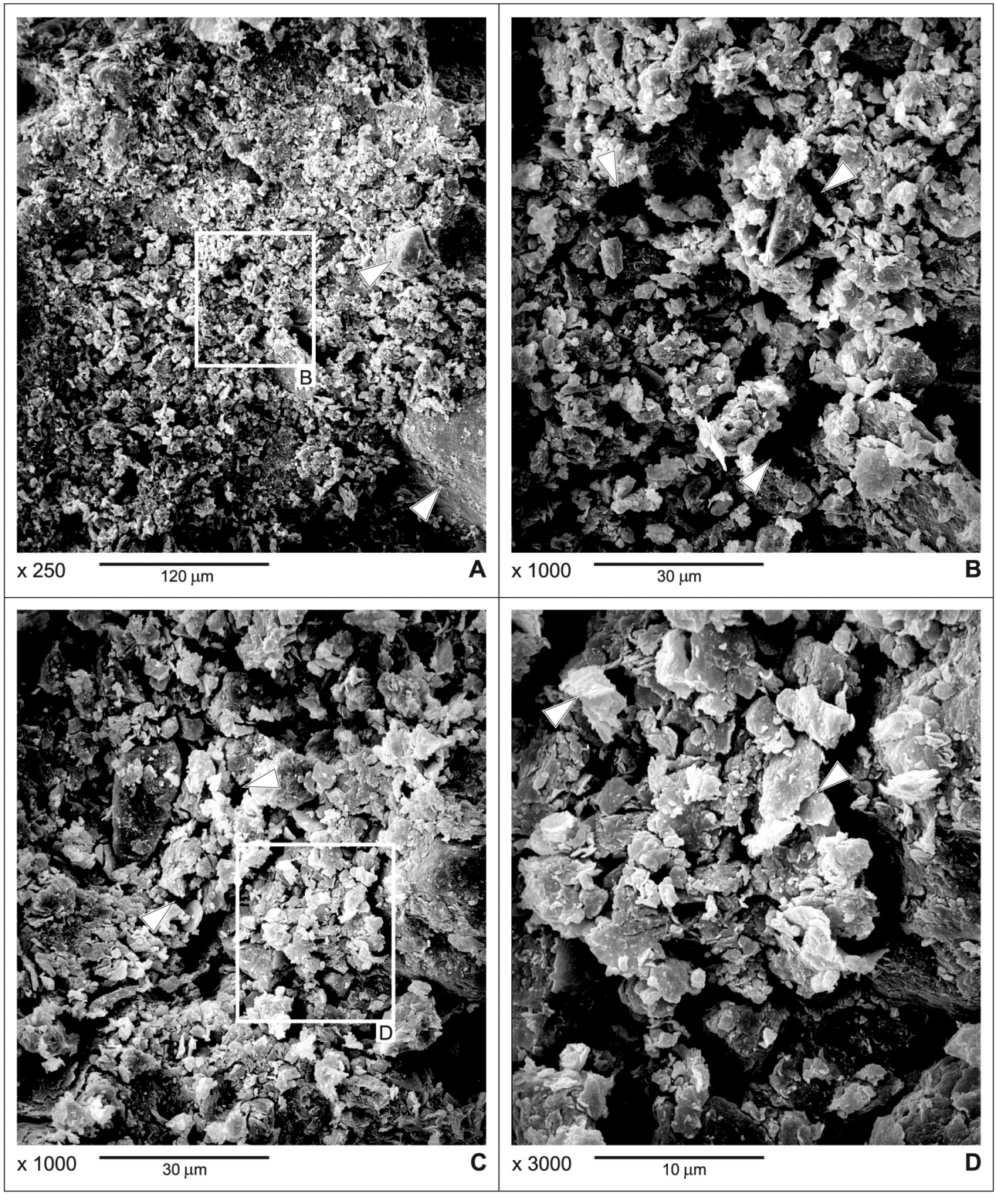

Fig. 3. Scanning electron photomicrographs of the matrix microstructure (subtype B). Microstructure of till from exposure number 30, location in Fig. 1. Orientation: S–N (S – left part of the photos). *A* – sandy and fine silty grains (arrows) within clayey matrix. Structural elements of the microstructure are medium packed. The pore space is formed by isometric and anisometric small mesopores among the aggregates (black areas); *B* – enlarged detail of A: medium packed clayey and silty-clayey microaggregates. Note anisometric mesopores (lower arrow) and intermicroaggregate isometric and anisometric micropores (upper arrows); *C* – medium packed clayey and silty-clayey microaggregates; pore space of matrix formed by isometric and anisometric intermicroaggregate micropores (arrows); *D* – enlarged detail of C: face-to-edge contacts (arrows) among clayey microaggregates

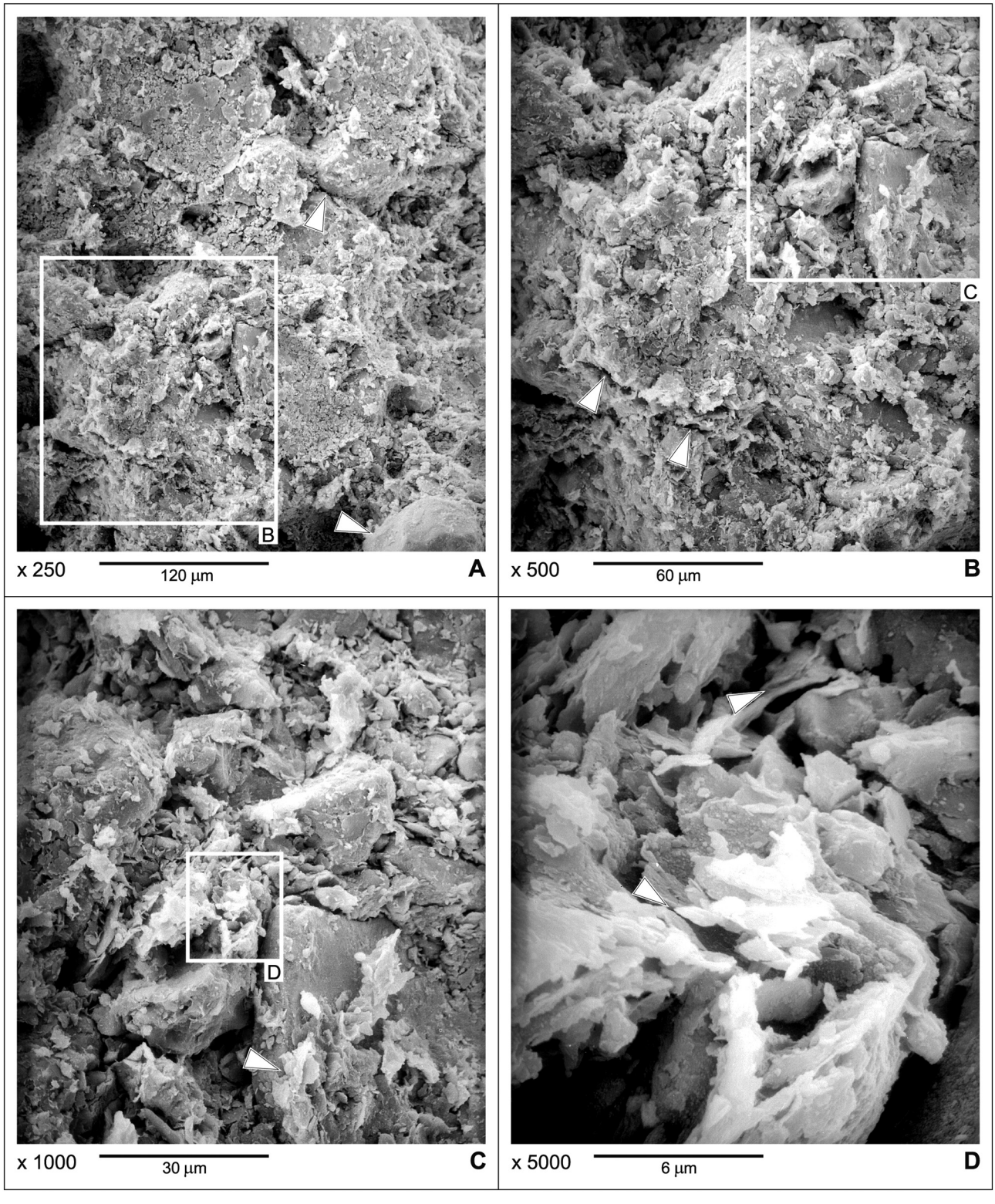

Fig. 4. Scanning electron photomicrographs of the matrix microstructure (subtype C). Microstructure of till from exposure number 31, location in Fig. 1. Orientation: W–E (W – left part of the photos). *A* – sandy and silty grains (arrows) within clayey matrix, closely linked with it. The pore space is formed by small anisometric mesopores (black areas) between aggregates; *B* – enlarged detail of A: tightly packed sandy-clayey and silty-clayey aggregates. The matrix pore space is formed mainly by anisometric intermicro-aggregate micropores (arrows); *C* – enlarged detail of B: surface of silty grain is covered by thin film of clayey microaggregates and particles (arrow); *D* – enlarged detail of C: face-to-face contacts between clayey microaggregates (arrows)

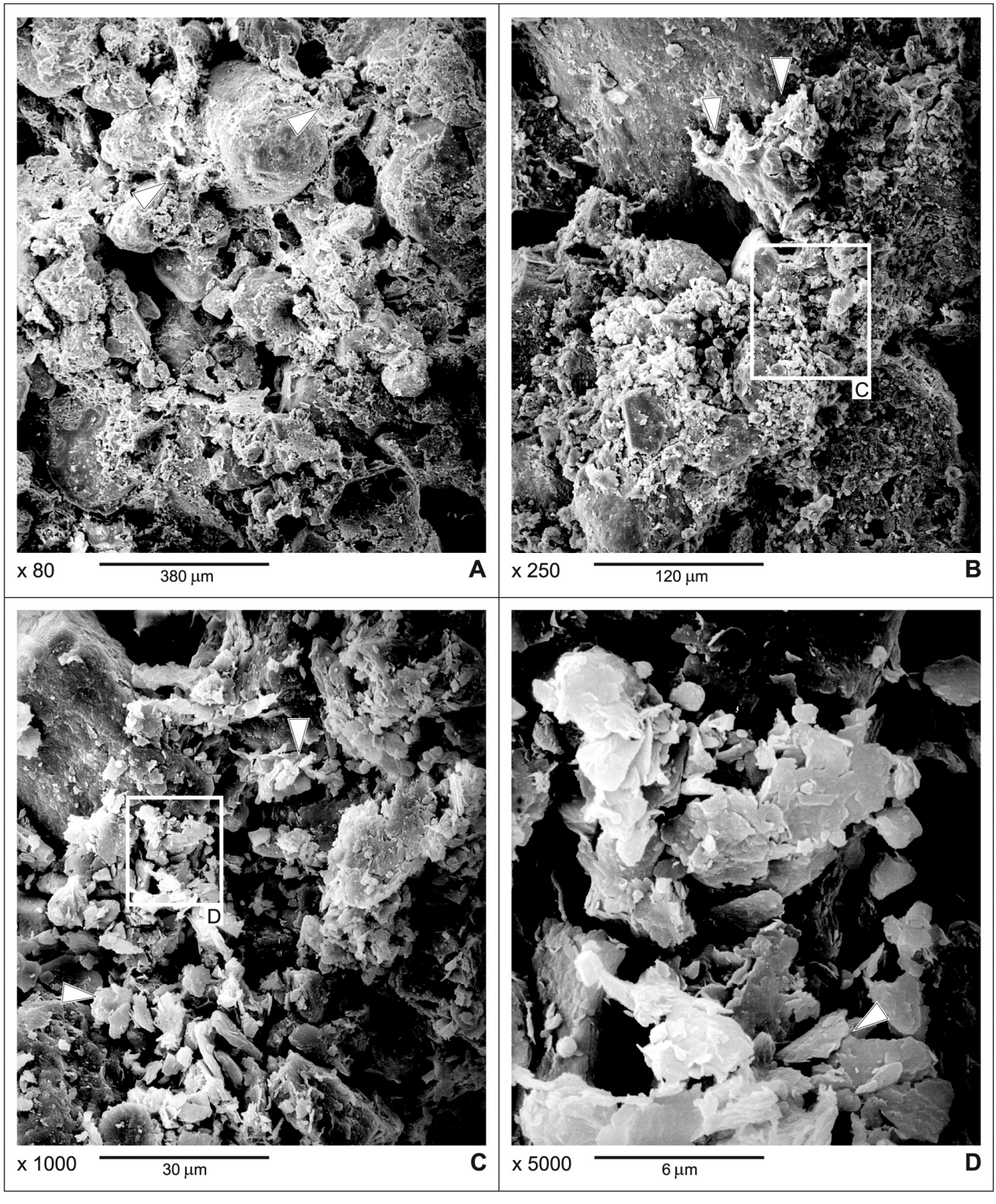

Fig. 5. Scanning electron photomicrographs of the skeletal microstructure. Microstructure of till from exposure number V/66, location in Fig. 1. Orientation: W–E (W – left part of the photos). *A* – unevenly distributed clay and fine silt material between the skeleton composed of sandy and coarse silty grains. The clayey and silty-clayey aggregates and microaggregates form connectors between the skeleton sandy grains (arrows). The pore space is formed mainly by intergranular large isometric and anisometric mesopores (black areas); *B* – fragment of sandy grain (upper part of photo-arrows) with loosely attached silty-clayey aggregates (fragment of connector among grains); *C* – enlarged detail of B: loosely packed and unevenly distributed silty grains (upper left part of the photo) and clayey microaggregates (arrows). The pore space is formed by anisometric intermicro-aggregate micropores (black areas); *D* – enlarged detail of C: face-to-edge contacts between clayey microaggregates (arrow)

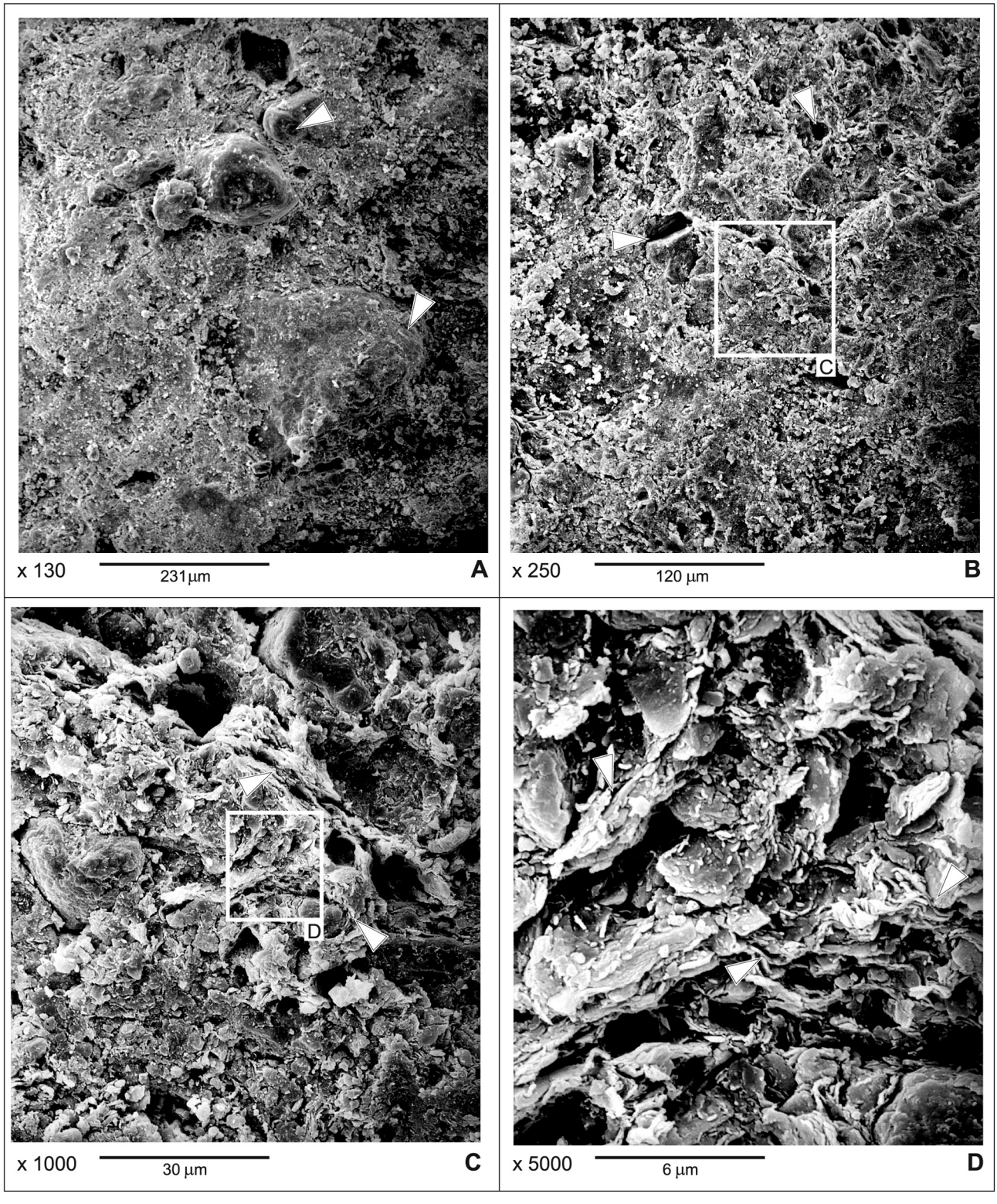

Fig. 6. Scanning electron photomicrographs of the matrix-turbulent microstructure. Microstructure of till from exposure number IX/69, location in Fig. 1. Orientation: W–E (W – left part of the photos). *A* – sandy and silty grains (arrows) in clayey matrix; sandy grain very closely covered by "clay film" (lower arrow). Note that the matrix fills the space among the grains very tightly and adheres tightly to their surface. The pore space is formed by small isometric and anisometric mesopores (black areas) among aggregates; *B* – clayey matrix formed by tightly packed clayey and silty-clayey microaggregates. Pore space of matrix formed by anisometric intermicroaggregate micropores (arrows), *C* – enlarged detail of B: "clay film" (lower arrow) around silty grain. A discontinuity plane is present above, along which face-to-face contacts among clayey microaggregates occur (upper arrow); *D* – enlarged detail of C: turbulent arrangement (arrow in the right side of the photo) of clayey microaggregates. Note face-to-face (upper left arrow) and face-to-edge at small angle (lower left arrow) contacts between microaggregates

Table 3. **Relation of the physical properties of tills (free swell, final water content of free swell, slaking) to types / subtypes of their microstructures (explanations in Table 2)**

Microstructures Type / Subtype			Free swell FS, %	Final water content of free swell w_f, %	Slaking SL, %		Time of slaking t_{SL}, hour	
					Natural water content	Hygroscopic moisture	Natural water content	Hygroscopic moisture
Skeletal		R	0.0–1.6	17.3–31.9	50–100	79–100	0.1–24.0	0.01–24.0
		$\overline{X}$	0.6	24.3	81	98	12.2	2.6
Matrix	A	R	0.1–12.7	16.4–36.5	18–100	67–100	0.17–24.0	0.02–24.0
		$\overline{X}$	2.2	24.2	77	97	16.8	4.1
	B	R	0.0–6.7	12.4–35.7	2–100	31–100	0.05–24.0	0.02–24.0
		$\overline{X}$	1.2	21.5	76	93	13.5	4.8
	C	R	0.0–11.7	13.6–30.2	7–100	15–100	0.5–24.0	0.02–24.0
		$\overline{X}$	1.5	18.9	61	78	18.3	10.8
Matrix–turbulent		R	0.0–0.5	15.8–21.0	3–100	17–100	12.0–24.0	0.9–24.0
		$\overline{X}$	0.2	17.6	36	56	21	18.2

Table 4. **Relation of the mechanical properties of tills (oedometer and consolidometer modulus) to types / subtypes of their microstructures (explanations in Table 2)**

Microstructures Type / Subtype			Oedometer modulus M_o, MPa			Consolidometer modulus M_c, MPa		
			Load, MPa			Load, MPa		
			0.1	0.2	0.4	0.1	0.2	0.4
Skeletal		R	5.4–48.6	4.5– 27.4	4.3–61.2	3.0–15.2	4.2–17.3	7.4–32.6
		$\overline{X}$	16.1	13.9	24.8	6.9	9.4	15.8
Matrix	A	R	3.7–25.7	3.1–33.9	2.9–396.0	1.6–21.3	2.8–27.2	4.8–38.9
		$\overline{X}$	13.1	17.3	45.5	8.1	10.8	15.6
	B	R	3.5–42.3	2.9–50.8	2.5–80.6	1.8–37.2	3.0–44.5	5.4–52.3
		$\overline{X}$	16.7	18.5	26.6	10.7	14.4	19.8
	C	R	4.0–180.6	10.8–190.4	10.2–185.6	3.5–101.5	5.7–120.5	9.7–140.3
		$\overline{X}$	49.7	59.3	65.3	30.5	35.1	47.7
Matrix–turbulent		R	25.1–71.8	29.4–95.7	44.1–130.5	21.4–58.2	27.8–49.6	36.5–81.2
		$\overline{X}$	44.3	49.2	75.3	36.5	38.1	53.5

Table 5. **Relation of the mechanical properties of tills (angle of shear resistance and apparent cohesion) to types / subtypes of their microstructures (explanations in Table 2)**

Microstructures Type / Subtype			Shearbox test		Triaxial compression test			
					Total stress		Effective stress	
			φ, °	c, kPa	φ, °	c (kPa)	φ, °	c, kPa
Skeletal		R	13.1–24.7	21.0–93.6	6.2–19.5	15.0–78.6	15.6–22.5	14.0–70.4
		$\overline{X}$	21.1	46.7	13.2	38.3	19.9	33.1
Matrix	A	R	14.5–35.5	18.0–122.8	6.0–27.5	16.0–101.3	11.5–32.0	12.5–95.6
		$\overline{X}$	22.9	47.1	15.1	37.0	20.3	34.5
	B	R	15.5–32.0	13.5–138.5	8.0–25.6	0.5–121.3	13.0–28.5	2.0–117.3
		$\overline{X}$	23.4	47.0	16.4	39.5	21.0	36.5
	C	R	18.0–40.5	36.0–160.3	8.5–32.0	37.5–153.0	17.0–35.5	30.5–145.2
		$\overline{X}$	30.7	79.3	22.6	70.2	27.2	64.9
Matrix–turbulent		R	21.4–29.0	40.5–181.5	15.3–23.5	39.0–153.2	19.8–27.5	35.5–140.1
		$\overline{X}$	25.6	105.8	20.6	86.5	23.7	79.0

φ – angle of shear resistance, c – apparent cohesion.

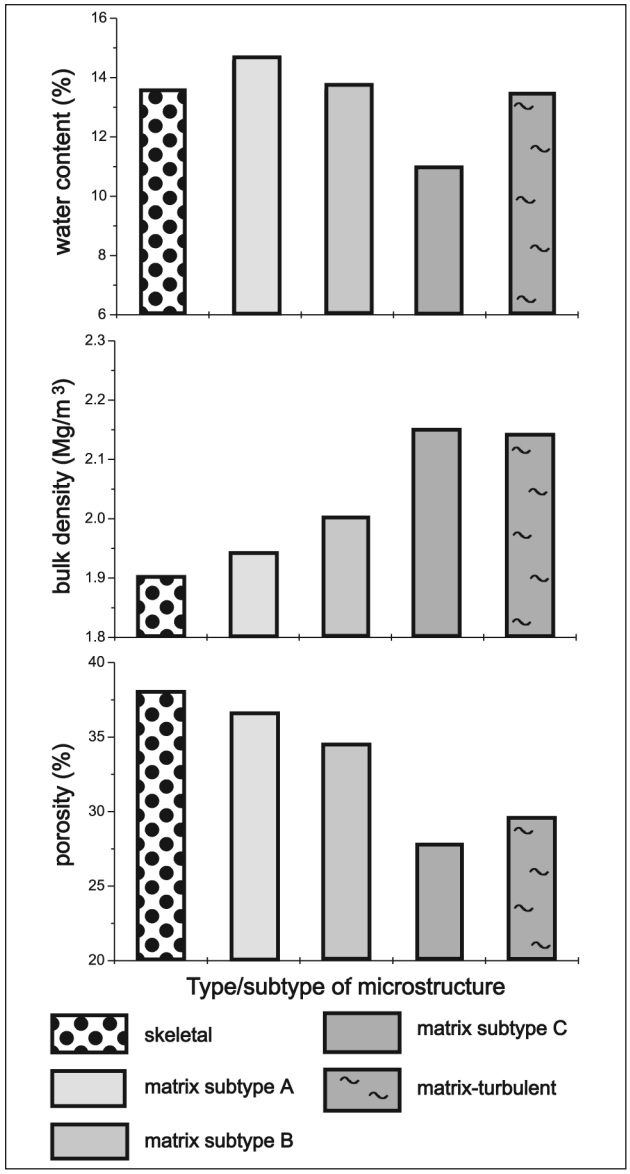

Fig. 7. Relation between selected physical properties of tills (water content, bulk density, porosity) and their microstructure

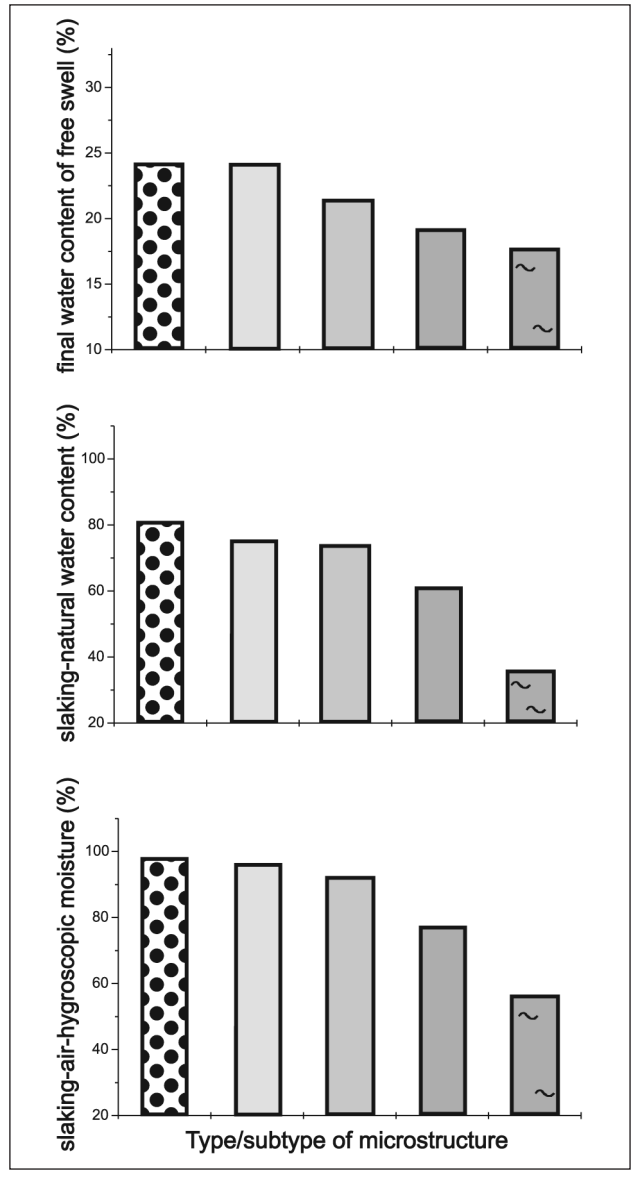

Fig. 8. Relation between selected physical properties of tills (final water content of swell, slaking) and their microstructure (explanations in Fig. 7)

Water content, density, porosity

The obtained results are presented in Table 2 (water content, bulk density, dry density, porosity and void ratio) and in Fig. 7 (water content, bulk density and porosity).

The highest variability of water content occurs in tills with the skeletal microstructure (6.1% to 25.9%). For tills with the matrix microstructure, the average water content changes from subtype A (14.6%) to subtype C (10.9%). The coefficient of variation varies between 10% and 39%. The lowest variability of water content is noted in tills with the matrix-turbulent microstructure (12.1% to 15.3%).

In tills with the skeletal microstructure, the average bulk density is lowest (1.90 mg/m^3) and increases in tills with the matrix microstructure from subtype A (1.94 mg/m^3) to subtype B (2.00 mg/m^3). A particularly large increase of this parameter is observed in tills with the subtype C matrix (2.15 mg/m^3) and matrix-turbulent microstructures (2.14 mg/m^3). The coefficient of variation is low (between 1% and 6%). Similar trends are noted for the dry density values. Only in the case of tills with the matrix-turbulent microstructure the average value of this parameter is much lower (1.88 mg/m^3) in comparison to tills with the subtype C matrix microstructure. The coefficient of variation is low and varies between 1% and 8%.

In tills with the skeletal and matrix microstructures (subtype A and B), the porosity values lie within the same range (between 24.7% and 47.4%), whereas the average value is highest in tills with the skeletal microstructure (38.0%). In tills with the matrix microstructure, the porosity values decrease from subtype A (36.4%) to subtype C (27.8%). Also, in tills with the matrix-turbulent microstructure the parameter reaches lower average values (29.3%) than in the subtype C matrix microstructures. The coefficient of variation varies from 10% to 16%. Similar trends were noted for the void ratio values.

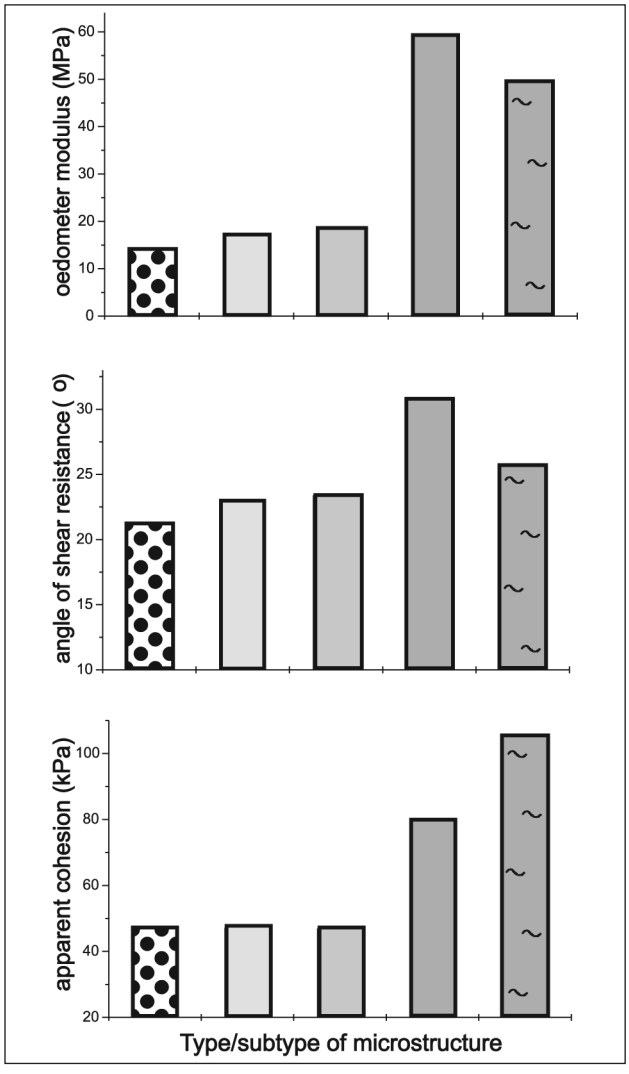

Fig. 9. Relations between selected mechanical properties of till (oedometer modulus-load 0.2 MPa, angle of shear resistance-shearbox test, apparent cohesion-shearbox test) and their microstructure (explanations in Fig. 7)

Swelling and slaking

The obtained results are presented in Table 3 (free swell, final water content of free swell, slaking and the time of slaking for natural water content and hygroscopic moisture) and in Fig. 8 (final water content of free swell, slaking for natural water content, slaking for hygroscopic moisture).

Free swell was analysed on samples of tills with natural water content. Tills with the skeletal and matrix-turbulent microstructure show the lowest swelling (1.6% at the maximum). The values of this parameter increase in tills with the matrix microstructure – maximally up to 12.7%. In tills with the matrix microstructure, the average value of the final water content of swelling decreases from subtype A (24.2%) to subtype C (18.9%).

The analysis of slaking was carried out on samples with natural water content and hygroscopic moisture; the results are shown in Table 3 and Fig. 8. Tills with the skeletal microstructure have the highest degree of slaking in samples with a natural water content (81% on the average). In tills with the subtype A matrix microstructure the average value is 77%, and it decreases to 61% in subtype C. A particularly large decrease of this parameter (to 36%) is observed in tills with the matrix-turbulent microstructure. The degree of slaking in tills with hygroscopic moisture is much higher in comparison to values obtained for samples with natural water content; nevertheless, they indicate a similar tendency. The coefficient of variation lies between 6% and 71%.

The time of slaking for tills (with a natural water content) with the skeletal microstructure is the shortest (12.2 h on the average). The average slaking time for tills with the matrix microstructure varies between 13.5 h for subtype B and 18.3 h for subtype C. In turn, the slaking time for tills with the matrix-turbulent microstructure is the longest and reaches an average of 21 h. The slaking time for tills with hygroscopic moisture is much shorter than that for tills with natural water content. The general tendency is nevertheless similar to that observed for tills with natural water content. The coefficient of variation lies between 63% and 288%.

Compressibility and shear strength

The obtained results are presented in Table 4 (oedometer modulus, consolidometer modulus), Table 5 (angle of shear resistance and apparent cohesion for shearbox test and triaxial compression test) and Fig. 9 (oedometer modulus, angle of shear resistance and apparent cohesion).

In laboratory conditions, the analyses of tills in one-dimensional deformation states were carried out in an oedometer and a consolidometer. The compressibility moduli obtained in oedometers were higher in comparison to those obtained in consolidometers. For tills with the skeletal microstructure, the average value of the modulus was generally the lowest. In tills with the matrix microstructure, the average values of the modulus increased from subtype A to subtype C. For tills with the matrix-turbulent microstructure, the parameter attains similar values as for tills with the subtype C matrix microstructure.

The shear strength was tested in a shearbox apparatus and in a triaxial compression apparatus. Based on shear tests, the parameters of Coulomb's equation were determined: φ – the angle of shear resistance and *c* – cohesion. During analyses in the triaxial compression apparatus, φ and *c* were determined in total and effective stresses. For tills with the skeletal microstructure, the angle of shear resistance and cohesion attain the lowest values. In tills with the matrix microstructure, the values of these parameters increase from subtype A to subtype C. The average value of the angle of shear resistance in tills with the matrix-turbulent microstructure is slightly lower than in the case of tills with the subtype C matrix microstructure. The average values of cohesion for tills with the matrix-turbulent microstructure are among the highest.

INTERPRETATION OF RELATIONS BETWEEN PHYSICO-MECHANICAL PROPERTIES AND MICROSTRUCTURE

Intergranular large mesopores, intermicroaggregate micropores and face-to-edge contacts among clayey microaggregates (Fig. 5) result from the loose packing of the structural elements in tills of skeletal microstructure. As a consequence, relatively highest porosity and lowest bulk density values are noted for tills of this microstructure (Fig. 7). The factor possibly responsible for the

origin of such loose packing of the mineral skeleton is a high water content (Table 2) for such a low amount of clayey particles. This moisture is almost identical to the water content of tills with the matrix microstructure (subtypes A and B) in which the amount of clayey particles is significantly higher. It is, however, generally known that water content grows with the content of clayey particles. A high water content was responsible for the big distances between sandy and silty grains and the formation of long and loose clayey connectors. These connectors are built of clayey microaggregates with the face-to-edge type of contacts (Fig. 5A, B, D).

The increase of the packing of structural elements in tills with the matrix microstructure resulted in the shrinkage of the size of meso- and micropores, a change of their shape from isometric to more and more anisometric, as well as in the growing amount of face-to-face contacts between the clayey microaggregates (Fig. 2–4). This caused a drop of porosity and a growth of bulk density in tills with subtype A to C matrix microstructure (Fig. 7). Such a situation could have been caused, among others, by a decrease of moisture, considerable particularly in tills with the subtype C matrix microstructure. The low water content permitted a reduction of the distance among the structural elements and an increasingly closer face-to-face contacts among clayey aggregates. The clay films around the sandy grains and the clayey connectors could therefore be more tightly connected with their surface (Fig. 4C).

A slight loosening of packing of the structural elements in the matrix-turbulent microstructure could result from the turbulent distribution of clayey microaggregates in the clayey matrix and, consequently, the formation of face-to-edge contacts at a small angle among them (Fig. 6). Therefore, as compared with tills of subtype C matrix microstructure, a slight growth of porosity and a drop of bulk density are noted in these tills (Fig. 7). Such a situation is due to the growth of water content in tills with the matrix-turbulent microstructure to a level usually noted in tills with the subtype B matrix and skeletal microstructure. However, the growth of porosity and a decrease of bulk density did not reach the level obtained for tills with such types of microstructure (Fig. 7). Most probably such a high moisture content could be acquired by tills with the matrix-turbulent microstructure due to a more extensive filling of pore space with water. This extensive filling of pore space with water can be responsible also for the turbulent distribution of clayey microaggregates, which in such an environment could behave in a more elastic manner enabling the turbulent distribution.

The increase of the packing degree of the structural elements, the shrinking of pore size and the increasingly frequent face-to-face contacts in tills with a microstructure varying from skeletal to matrix-turbulent continuously limited the possibilities of water entering their structure and thus led to a drop of the final water content of free swell and slaking of tills (Fig. 8). A possible factor additionally hindering the free swell and slaking of tills with the densely packed microstructure were structural bonds stronger than in tills with the loosely packed microstructure. The relatively lower value of these parameters in tills with the matrix-turbulent microstructure may result from the turbulent distribution of clayey microaggregates in this microstructure (Fig. 6D), which additionally limited the penetration of water into this structure.

Due to a high porosity and moisture content, a relatively highest compressibility and the lowest shear strength are noted in tills with the skeletal and matrix subtype A and B microstructure. In these tills, compression led to a displacement of grains and particles, a closure of big mesopores and micropores and a removal of water and air from the pore space. All these factors resulted in considerable lateral displacements and, consequently, in high compressibility values (Table 4 and Fig. 9). During the shearing process, large distances among the structural elements, loose contacts, mainly of face-to-edge type, as well as unstable structural bonds caused a minor structural resistance in these tills and the relatively lowest shear strength.

The shrinking of pores and changes of shape from isometric to anisometric, the increasingly closer face-to-face and face-to-edge at a small angle contacts and more stable contacts among the structural elements led to the growth of shear strength and a lower compressibility in tills with the matrix microstructure, subtype C and matrix-turbulent microstructure (Tables 4, 5 and Fig. 9). All these changes were responsible for the drop of porosity and moisture content values.

CONCLUSIONS

The study tills are characterised by three types of microstructures: skeletal, matrix and matrix-turbulent. In the predominant matrix microstructure, three subtypes were distinguished according to the packing degree: loose – subtype A, medium – subtype B, and tight – subtype C. In tills with the skeletal microstructure, structural elements are loosely packed, while in the matrix-turbulent microstructure the packing is tight.

The physico-mechanical properties of tills are extremely variable, even within tills with the same microstructure. There are, however, distinct relations between these properties and the type / subtype of microstructure. Decrease of water content, porosity, soaking and compressibility, with a parallel increase of bulk density, swelling and shear strength, are observed in tills with the skeletal microstructure through tills with the matrix microstructure and those with the matrix-turbulent microstructure (Fig. 7–9). Analysis of some microstructural features such as the size and shape of pores, types of contacts and their stability, as well as the degree of packing of the structural elements suggests that the reason for their variability is the differentiated amount of water contained in tills. Changes in the water content and the microstructural features examined are responsible for the varying values of some physical and mechanical properties.

ACKNOWLEDGEMENTS

The author is grateful to Barbara Grabowska-Olszewska, Hanna Ruszczyńska-Szenajch (Faculty of Geology, University of Warsaw) and Jan A. Piotrowski (Department of Earth Sciences, University of Aarhus) for their editorial suggestions concerning the former draft of this paper. I thank also Ryszard Orłowski (Polish Academy of Sciences, Institute of Geological Sciences – SEM & Electron Probe Microanalysis Laboratory) for his help in laboratory investigations and Piotr Sztandar-Sztanderski (Medgraf Ltd.) for technical preparation of the illustrations.

References

1. Dobak P. 1986. Zmiany odkształcalności gruntów wywołane procesami inżyniersko-geologicznymi w rejonie kopalni węgla brunatnego „Bełchatów". Rozprawa doktorska. Warszawa, Wydział Geologii, Uniwersytet Warszawski.
2. Falkiewicz A. 1962. Własności fizyczno-mechaniczne glin zwałowych środkowego Mazowsza. *Biuletyn Geologiczny UW*. ***2***. 3–128.
3. Grabowska-Olszewska B., Osipov V. I., Sokolov V. N. 1984. Atlas of the microstructure of clay soils. Warszawa: Państwowe Wydawnictwo Naukowe. 414 p.
4. Grabowska-Olszewska B., Kaczyński R. 1994. Metody badania pęcznienia gruntów spoistych. *Gospodarka Surowcami Mineralnymi*. ***10***(*1*). 125–160.
5. Gratchev I. B., Sassa K., Osipov V. I., Sokolov V. N. 2006. The liquefaction of clayey soils under cyclic loading. *Engineering Geology*. ***86***. 70–84.
6. Kaczyński R. 1981. Wytrzymałość i odkształcalność górnomioceńskich iłów zapadliska przedkarpackiego. *Biuletyn Geologiczny UW*. ***29***. 105–193.
7. Kaczyński R., Trzciński J. 1992. The physical-mechanical and structural properties of boulder clays of the Vistula Glaciation in the area of Poland. *Geological Quarterly*. ***36***(*4*). 481–508.
8. Kaczyński R., Trzciński J. 1999. Microstructural nonhomogeneity of glacial tills. *Visnyk Lviv. Univ. Ser. Mech. Math*. ***55***. 152–157.
9. Kaczyński R., Trzciński J. 2000. Geotechnical and microstructural parameters of glacial tills from the northern part of Poland. In: Mets D. M. (ed.). *Baltic Geotechnics IX 2000, Proceedings of the Ninth Baltic Geotechnical Conference*. Tallinn: A. A. Balkema. Rotterdam–Brookfield. 35–39.
10. Kowalski W. C., Lipińska N. 1963. Rodzaje gruntów serii glin zwałowych Warszawy. *Przegląd Geologiczny*. ***9***(*126*). 426–429.
11. Krajewska-Pinińska J. 1969. Inżyniersko-geologiczna charakterystyka glin zwałowych w nadkładzie węgla brunatnego okolic Turka. *Biuletyn Geologiczny*. ***11***. 101–154.
12. Lindner L. 1984. An outline of Pleistocene chronostratigraphy in Poland. *Acta Geologica Polonica*. ***34***(*1–2*). 27–49.
13. Mitchell J. K. 1993. Fundamentals of Soil Behaviour. New York: John Wiley & Sons, Inc. 437 p.
14. Osipov V. I., Nikolaeva S. K., Sokolov V. N. 1984. Microstructural changes associated with thixotropic phenomena in clay soils. *Géotechnique*. ***34***. 293–303.
15. Piaskowski A. 1989a. Wytyczne oznaczania modułów ściśliwości i współczynników konsolidacji gruntów metodą konsolidometryczną. ITB instrukcja Nr 288. Warszawa.
16. Piaskowski A. 1989b. Wytyczne wyznaczania modułów ściśliwości i odprężenia gruntów metodą edometryczną. ITB instrukcja Nr 289. Warszawa.
17. Polska Norma 1988. Grunty budowlane. Badania próbek gruntu. PN-88/B-04481. Warszawa.
18. Ruszczyńska-Szenajch H., Trzciński J. and Jarosińska, U. 2003. Lodgement till deposition and deformation investigated by macroscopic observation, thin section analysis, and electron microscope study. *Boreas*. ***32***. 399–415.
19. Scott R. E. 1961. New method of consolidation coefficient evaluation. *Journal ASCE*. ***87*** (SM1).
20. Sergeyev Y. M., Grabowska-Olszewska B., Osipov V. I., Sokolov V. N., Kolomenski Y. N. 1980. The classification of microstructures of clay soil. *Journal of Microscopy*. ***120***. 237−260.
21. Smart P., Tovey K. 1982. Electronmicroscopy of Soils and Sediments: Techniques. Oxford: Clarendon Press. 264 p.
22. Sztromajer Z. 1982. Właściwości fizyczne górnych glin zwałowych Łodzi. *Biuletyn Geologiczny UW*. ***27***. 139–192.
23. Trzciński J. 1998. Mikrostruktury a właściwości geologiczno-inżynierskie glin lodowcowych. Rozprawa doktorska. Warszawa, Wydział Geologii, Uniwersytet Warszawski.
24. Trzciński J. 2003. Mikrostruktury glin lodowcowych badane w skaningowym mikroskopie elektronowym. In: Harasimiuk M., Terpiłowski S. (eds.). *Analizy sedymentologiczne osadów glacigenicznych*. Lublin: Wydawnictwa Uniwersytetu Marii Curie-Skłodowskiej. 63–77.
25. Trzciński J. 2004. Combined SEM and computerized image analysis of clay soil microstructure: technique & application. In: Jardine R. J., Potts D. M., Higgins K. G. (eds.). *Advances in Geotechnical Engineering. The Skempton Conference*. London: Thomas Telford. 654–666.
26. Trzciński J., Kaczyński R. 1999. Nonhomogeneity of the physical properties of glacial tills. *Visnyk Lviv. Univ. Ser. Mech. Math*. ***55***. 158–160.
27. Vu Cao Minh, Glazer Z. 1977. Nowa metoda wyznaczania edometrycznego modułu ściśliwości ogólnej. *Inżynieria i Budownictwo*. ***1***(*385*). 25–28.
28. Wysokiński L. 1967. Wpływ spękań w glinach zwałowych na stateczność skarpy wiślanej w Płocku na tle analizy aktualnych powierzchniowych ruchów masowych. *Biuletyn Geologiczny UW*. ***9***. 129–216.

Jerzy Trzciński

MORENINIO PRIEMOLIO MIKROSTRUKTŪROS IR FIZIKINĖS MECHANINĖS SAVYBĖS

S a n t r a u k a

Straipsnyje pateikiami mikrostruktūrų tyrimo, naudojant nuskaitantį elektroninį mikroskopą (SEM), rezultatai, taip pat Lenkijos moreninio priemolio fizikinės mechaninės savybės. Ištirta struktūrinių elementų sanglauda, kontaktų tarp atskirų elementų stiprumas, kontaktų tarp molio mikroagregatų rūšys bei porų forma ir dydis. Tiriamame moreniniame priemolyje nustatyti trys mikrostruktūros tipai: karkasinis, štampinis ir štampinis-turbulentinis. Atsižvelgiant į struktūrinių elementų sanglaudą, dažniausiai aptinkamoje štampinėje mikrostruktūroje išskirti trys porūšiai: A (puri), B (vidutinė) ir C (tanki). Įrodytas ryšys tarp atskirų mikrostruktūros rūšių ir fizikinių mechaninių savybių. Drėgnumo, poringumo, deformacijos vertės mažėja šia kryptimi: karkasinė mikrostruktura – štampinė – štampinė-turbulentinė, o tankio brinkumo, kerpamojo stiprio vertės minėta kryptimi didėja. Sąsajų tarp mikrostruktūros ir fizikinių mechaninių savybių analizė patvirtina tiesioginį vandens kiekio porose poveikį sąsajoms.

Jerzy Trzciński

MIKROSTRUKTURY I WŁAŚCIWOŚCI FIZYKO-MECHANICZNE GLIN LODOWCOWYCH Z POLSKI

Streszczenie

Wykonano badania mikrostruktur z zastosowaniem skaningowego mikroskopu elektronowego (SEM) oraz właściwości fizyko-mechanicznych glin lodowcowych z Polski. Określono następujące cechy mikrostruktury: stopień upakowania elementów strukturalnych, wytrzymałość na kontaktach pomiędzy elementami strukturalnymi, typy kontaktów pomiędzy mikroagregatami ilastymi oraz wielkość i kształt porów. W badanych glinach lodowcowych występują trzy typy mikrostruktur: szkieletowa, matrycowa i matrycowo-turbulentna. W obrębie najczęściej występującej mikrostruktury matrycowej wydzielono trzy podtypy ze względu na upakowanie elementów strukturalnych: podtyp A (luźno upakowana), podtyp B (średnio upakowana) i podtyp C (ciasno upakowana). Znaleziono związki pomiędzy typem/podtypem mikrostruktury a zbadanymi parametrami fizyko-mechanicznymi. Spadła wartość wilgotności, porowatości, rozmakania i ściśliwości oraz wzrosła gęstość objętościowa, pęcznienie i wytrzymałość na ścinanie od glin o mikrostrukturze szkieletowej przez gliny o mikrostrukturze matrycowej do glin o mikrostrukturze matrycowo-turbulentnej. Analiza związków pomiędzy fizyko-mechanicznymi właściwościami glin a ich mikrostrukturami ujawniła, że zawartość wody w przestrzeni porowej i niektóre cechy mikrostruktur mają wpływ na te relacje.

Ежи Трчиньски

МИКРОСТРУКТУРЫ И ФИЗИКО-МЕХАНИЧЕСКИЕ СВОЙСТВА МОРЕННЫХ СУГЛИНКОВ

Резюме

Приводятся результаты исследования микроструктур, осуществленного с помощью сканирующего электронного микроскопа (SEM). Представлены физико-механические свойства моренных суглинков Польши. Исследовались упаковка структурных элементов, прочность контактов между ними, виды контактов, форма и величина пор. В моренных суглинках выявлены три типа микроструктур: каркасный, штамповый и штампово-турбулентный. Чаще встречается штамповая микроструктура. В ней выделены три вида: А (рыхлая упаковка), Б (упаковка средней плотности) и С (плотная упаковка). Доказана связь между типами микроструктур и физико-механическими свойствами. Значения таких показателей, как влажность, пористость, деформируемость, уменьшаются при переходе от каркасной микроструктуры к штамповой и штампово-турбулентной, а плотность, набухаемость, сопротивление сдвигу соответственно увеличиваются. Анализ результатов показал, что количество воды в поровом пространстве оказывает прямое влияние на указанные взаимосвязи.